

---

 **MG-LLaVA: Towards Multi-Granularity Visual Instruction Tuning**

---

Xiangyu Zhao<sup>1,2\*</sup>, Xiangtai Li<sup>2,3</sup>, Haodong Duan<sup>2</sup>, Haian Huang<sup>2</sup>,  
Yining Li<sup>2</sup>, Kai Chen<sup>2†</sup>, Hua Yang<sup>1†</sup>

<sup>1</sup>Shanghai Jiaotong University <sup>2</sup>Shanghai AI Laboratory

<sup>3</sup>S-Lab, Nanyang Technological University

**Project Page:** <https://phoenixz810.github.io/MGLLaVA/>

### Abstract

Multi-modal large language models (MLLMs) have made significant strides in various visual understanding tasks. However, the majority of these models are constrained to process low-resolution images, which limits their effectiveness in perception tasks that necessitate detailed visual information. In our study, we present MG-LLaVA, an innovative MLLM that enhances the model’s visual processing capabilities by incorporating a multi-granularity vision flow, which includes low-resolution, high-resolution, and object-centric features. We propose the integration of an additional high-resolution visual encoder to capture fine-grained details, which are then fused with base visual features through a Conv-Gate fusion network. To further refine the model’s object recognition abilities, we incorporate object-level features derived from bounding boxes identified by offline detectors. Being trained solely on publicly available multimodal data through instruction tuning, MG-LLaVA demonstrates exceptional perception skills. We instantiate MG-LLaVA with a wide variety of language encoders, ranging from 3.8B to 34B, to evaluate the model’s performance comprehensively. Extensive evaluations across multiple benchmarks demonstrate that MG-LLaVA outperforms existing MLLMs of comparable parameter sizes, showcasing its remarkable efficacy. The code will be available at <https://github.com/PhoenixZ810/MG-LLaVA>.

## 1 Introduction

Recent works on Multimodal Large Language Models (MLLMs) [1, 2, 3, 4, 5, 6] have achieved rapid development in vision language understanding, visual reasoning, visual interaction, and localization. Most MLLMs adopt pre-trained Large Language Models (LLMs) as the base architecture to process concatenated visual and language embeddings. As one representative work, LLaVA [3] adopts low-resolution ( $224^2$ ,  $336^2$ , *etc.*) images as inputs and aligns visual embeddings with the text modality via an MLP projector and then performs instruction tuning. The architecture of LLaVA has been widely adopted by subsequent works [7, 8, 9, 10], and has been applied to various vision tasks, including detection, segmentation, and video understanding.

Real-world images exhibit a wide range of resolutions, scales, and aspect ratios, posing significant challenges for MLLMs with low-resolution inputs in robustly processing them. To tackle this problem, recent works [11, 12, 8, 13, 14, 7, 15] have proposed various strategies to augment the capabilities of visual encoders in MLLMs, including training on diverse datasets, utilizing high-resolution image inputs, and employing dynamic aspect ratios. Most of these approaches involve the integration of

---

<sup>†</sup> Corresponding Author.

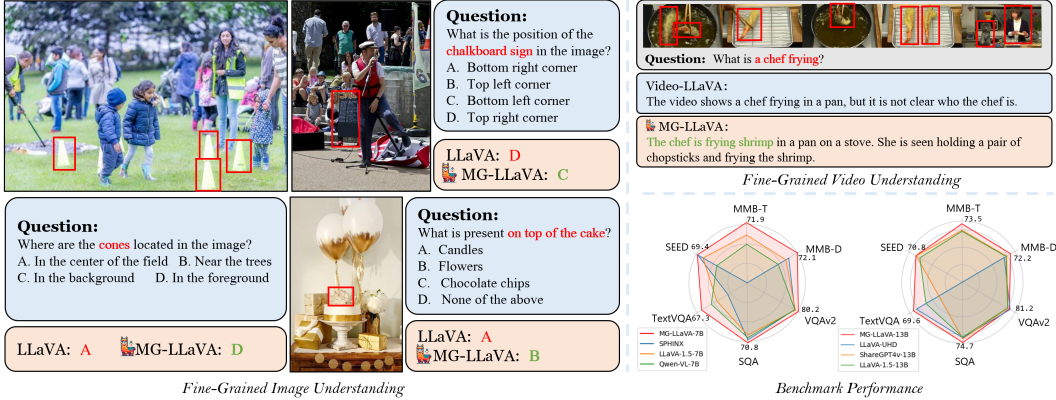


Figure 1: MG-LLaVA outperforms LLaVA across various vision-language tasks, particularly on tasks involving object recognition.

additional visual tokens through various techniques. Despite these advancements, two critical issues persist: (1) Although object-level features are crucial in nearly all visual understanding tasks, they are currently absent in existing vision encoders; (2) None of the existing MLLMs have integrated multi-granularity features, a classic concept in computer vision, into their frameworks.

Motivated by the aforementioned analysis, we introduce MG-LLaVA, a novel MLLM designed to effectively process multi-granularity visual inputs, including object-level, origin images, and high-resolution inputs. Our framework builds upon LLaVA [3] and is specifically tailored to incorporate and manage multi-granularity inputs. For object-level inputs, we employ a pre-trained open-vocabulary detector to identify object bounding boxes and execute RoI alignment to acquire region visual tokens. In contrast to close-set detectors, open-vocabulary detectors offer enhanced generalizability and robustness across diverse scenes. To handle fine-grained visual inputs, we utilize a convolution-based backbone [16] to extract richer visual features. Subsequently, we propose a straightforward yet effective fusion strategy to integrate these inputs into the original visual tokens in LLaVA. Specifically, we initially merge the fine-grained visual tokens with the original visual tokens using a simple Conv-Gate convolution, and then we append the object-level tokens to the fused tokens. Fig. 2 illustrate the difference between MG-LLaVA and existing MLLMs. Experimental results quantitatively validate the efficacy of the design of MG-LLaVA.

We perform extensive experiments with MG-LLaVA integrated with various language encoders, ranging from 3.8B to 34B, to substantiate the effectiveness of MG-LLaVA. Our evaluation encompasses 11 popular multimodal benchmarks for both image and video. Additionally, we present a comprehensive set of ablation studies that illustrate the impact of different components in MG-LLaVA. Benefiting from multi-granularity visual features, MG-LLaVA demonstrates a significantly enhanced capability in perception and visual comprehension, outperforming established counterparts and notably surpassing GPT-4V [17] and GeminiPro-V [18] on various multimodal benchmarks, including MMBench [19] and SEEDBench [20].

The contribution of this work can be summarized as follows:

- We introduce MG-LLaVA, an advanced multi-modal model adept at processing visual inputs of multiple granularities, including object-level features, original-resolution images, and high-resolution data. This advancement significantly enhances the capabilities of MLLMs in visual perception and understanding.
- We propose the Multi-Granularity Vision Flow, a straightforward yet effective module designed for the integration of features across various granularities, thereby significantly improving the performance of our model. The effectiveness of our approach is substantiated through empirical experiments.
- By employing a range of language models scaling from 3.8B to 34B, our model exhibits clear scalability and a marked proficiency in visual comprehension, outperforming established counterparts and notably surpassing GPT-4V and GeminiPro-V on MMBench and SEEDBench.

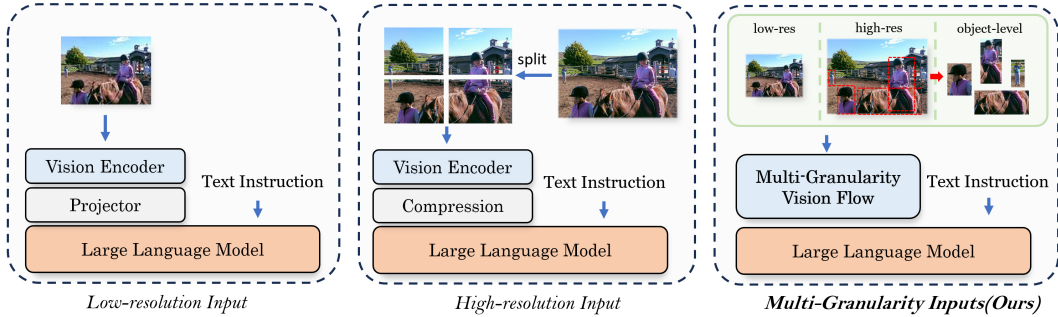


Figure 2: **Comparing Different MLLM Paradigms.** MG-LLaVA effectively perceives multi-granularity visual inputs that include object-level, low, and high-resolution inputs, thereby achieving advanced multi-modal understanding.

## 2 Related Work

**Large Language Models.** In recent years, private large language models (LLMs) like GPT-4 [17] and Llama [21] have gained remarkable performance. Concurrently, a multitude of open-source research [22, 23, 24, 25] has embarked on the exploration of LLMs. LLM shows strong performance in various NLP tasks. However, pure LLMs cannot handle image and video inputs. Our work focuses on designing new multimodal large language models, which jointly take visual and language tokens as inputs. In this work, we engaged a range of LLMs [22, 26, 27, 28] scaling from 3.8B to 34B. The observed performance across these models has proved the effectiveness of our design.

**Multimodal Large Language Models.** Multi-modal Large Language Models (MLLMs) [1, 2, 29, 30, 24, 31, 32, 10, 33, 34, 35] have recently showcased the potential to endow LLMs with visual conversational abilities. Among these models, LLaVA [31] typically built a simple architecture that utilizes a vision-language cross-modal adapter to bridge the gap between vision and language tokens. Some research [36, 37, 11] tried to increase performance by utilizing high-resolution inputs. LLaVA-UHD [7] cost-effectively increased input resolution by dividing high-resolution images into smaller slices. Subsequently, LLaVA-HR [14] and Mini-Gemini [8], endeavor to incorporate an additional visual encoder to enhance high-resolution details without increasing the count of visual tokens. However, these works consistently overlook the impact of fine-grained object-level features, which compromises their potential for enhanced perception. In comparison, MG-LLaVA explores the potential of multi-granularity input by simultaneously leveraging high-resolution inputs, low-resolution inputs, and object-level inputs. By flexibly integrating visual tokens of multiple granularity, MG-LLaVA achieves superior performance on several benchmarks with a marginal increase in cost.

**Multi-Granularity Modeling in Vision.** Inputs of multiple granularity have been incorporated into various downstream vision tasks. In object detection and segmentation, the efficacy of multi-level features has been well-established in detecting objects of different scales [38, 39, 40, 41, 42, 43, 44]. For panoptic segmentation, some methods [45, 46, 47, 48, 49, 50] applied a multi-granularity network to train instance, semantic, and part segmentation in parallel, and some studies [51, 52, 53, 54, 55] have indicated that training on various levels of abstraction can improve the performance of the segmentation network. For example, SAM [56] presents a multi-granularity mask prediction method for handling various level masks, such as things, background stuff, and parts. Motivated by the above works, we aim to capture input from various levels of perception into MLLM. In particular, we construct our model by developing multiple visual branches for different granularity, thereby augmenting its perceptual capabilities.

## 3 Method

In this study, we introduce MG-LLaVA, which effectively harnesses both the high-resolution and object-level features for the improvement of MLLMs. The architecture of MG-LLaVA is illustrated in Fig. 3. The model is composed of two key components: (1) Multi-Granularity Vision Flow framework for extracting visual features with different resolutions and granularities, while also

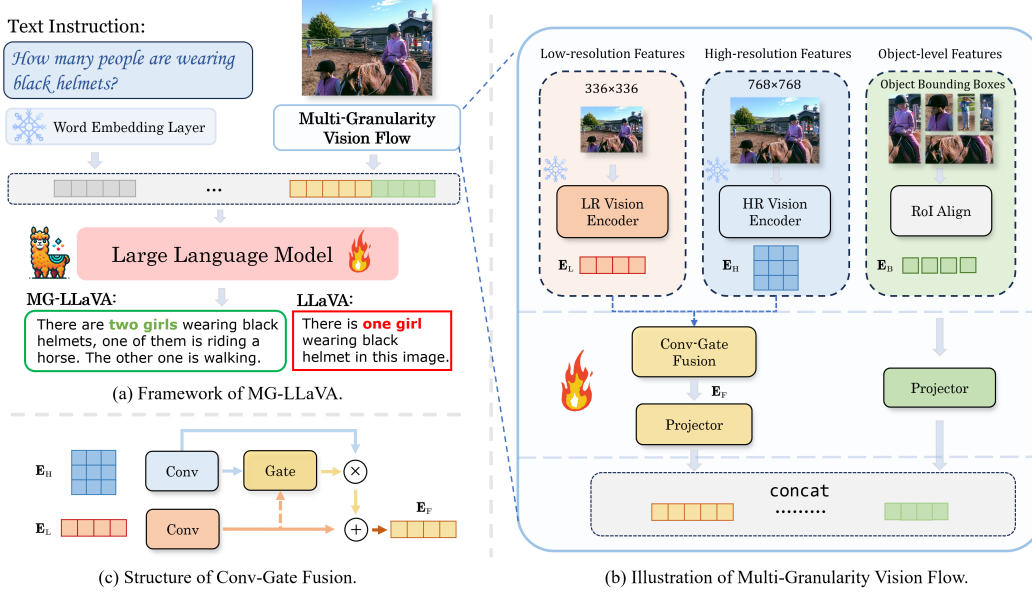


Figure 3: The illustration of MG-LLaVA. **Top left:** The overall framework of MG-LLaVA, which includes the Multi-Granularity Vision Flow module and a LLM. **Right:** Illustration of Multi-Granularity Vision Flow, which aims to extract multiple visual features and integrate disparate features to ensure seamless interaction. **Bottom left:** Structure of Conv-Gate Fusion module.

effectively integrating disparate features to ensure seamless interaction. (2) A large language model dedicated to generating coherent and contextually relevant responses.

### 3.1 Preliminary

As one of the most extensively adopted multi-modal LLM architectures, LLaVA consists of a vision encoder  $f_V$ , an MLP projector  $f_p$ , and a language model  $f_L$ . Given a visual input  $V$  and a textual input  $T$ , LLaVA computes the vision and language embeddings as per Eq. (1), where  $f_T$  represents the input embedding layer of  $f_L$ . The resulting embeddings,  $\mathbf{E}_T$  and  $\mathbf{E}_V$ , are then concatenated into a single token sequence, serving as the input to the LLM. LLaVA utilizes Eq. (2) to calculate the probability of the target answer  $\mathbf{X}_A$ , where  $\theta$  represents the trainable parameters and  $L$  is the length of  $\mathbf{X}_A$ . The model is trained on visual instruction tuning data to maximize  $p(\mathbf{X}_A | V, T)$ .

$$\mathbf{E}_T = f_T(T), \mathbf{E}_V = f_p(f_V(V)) \quad (1)$$

$$p(\mathbf{X}_A | V, T) = \prod_{i=1}^L p_{\theta}(\mathbf{X}_A^{[i]} | \text{Concat}(\mathbf{E}_V, \mathbf{E}_T^{[1:i-1]}), \mathbf{X}_A^{[i-1]}) \quad (2)$$

Despite the promising results, LLaVA still restrains itself in processing images at a low resolution ( $224^2$ ,  $336^2$ , etc.), which significantly hinders the model’s ability, particularly in the recognition of small objects. Scaling to high resolution without adapting the vision encoder directly would dramatically increase the number of visual tokens, rendering the approach ineffective. Furthermore, the visual input can also be complex and contain numerous objects within an image or video, which poses challenges for MLLMs in identifying some critical objects. Empirically, incorporating object-level features can significantly enhance the model’s perceptual abilities. Therefore, we introduce MG-LLaVA, which effectively harnesses both the high-resolution and object-level features for the improvement of MLLMs.

### 3.2 Multi-Granularity Vision Flow

**Hybrid Vision Encoders** As depicted in Fig. 3(b), MG-LLaVA initially processes images at two different resolutions: low-resolution  $V_L$  and high-resolution  $V_H$ . In the low-resolution branch, we follow the LLaVA-1.5 [31] to utilize a CLIP-pretrained ViT [57] denoted as  $f_V^L$  to derive low-resolution features  $\mathbf{E}_L \in \mathbb{R}^{N \times C}$ . The ViT feature  $\mathbf{E}_L$  benefits from an expanded receptive field, capturing a more comprehensive view of global information. In the high-resolution branch, we employ a CLIP-pretrained ConvNeXt [16] denoted by  $f_V^H$  to obtain high-resolution features  $\mathbf{E}_H \in \mathbb{R}^{h \times w \times C}$ .  $f_V^H$  effectively extracts detailed features from high-resolution images, offering detailed local insights.  $f_V^L$  and  $f_V^H$  downsample the input resolution with strides of 14 and 32, respectively. We therefore adjust  $V_L$  and  $V_H$  to ensure that the number of tokens in  $\mathbf{E}_L$  and  $\mathbf{E}_H$  remains the same ( $N = h \times w$ ).

**Conv-Gate Fusion** Combining both low and high-resolution features as inputs results in a doubling of the visual tokens to be processed, which is computationally ineffective. Moreover, the distinct architectures of ViT and ConvNeXt lead to a discrepancy between  $\mathbf{E}_L$  and  $\mathbf{E}_H$ , requiring a careful fusion process. Inspired from [14], we implement a lightweight Conv-Gate fusion network that facilitates feature aggregation while maintaining a single resolution’s token count, as shown in Fig. 3(c). We first employ 1D convolutions to align the channel widths of heterogeneous features and subsequently use a gating layer to modulate the semantic information across low and high resolutions, as described in Eq. (3). The fusion module is applied to the output of both vision encoders, resulting in only a marginal increase in computational cost.

$$\mathbf{E}_F = \mathbf{E}_L + G(\text{Conv}(\mathbf{E}_L), \text{Conv}(\mathbf{E}_H)) \times \mathbf{E}_H \quad (3)$$

**Integration of Object-level Features** Given the set of  $k$  object bounding boxes derived from the image, denoted as  $B = \{b_1, b_2, \dots, b_k\}$ , we employ the Region of Interest (RoI) Align to extract object-level features from the vision features of the high-resolution encoder  $f_V^H$ . Specifically, we upsample and concatenate features from different convolutional stages to a scale of 1/4 the input size, resulting in a multi-scale feature representation  $f_V^{H'}$ , which provides a fine-grained perspective. The object-level features are then aligned from  $f_V^{H'}$ . To maintain computational efficiency, we apply average pooling to each object feature and subsequently concatenate them into a sequence  $\mathbf{E}_B \in \mathbb{R}^{k \times C}$ , as detailed in Eq. (4).

$$\mathbf{E}_B = \text{Concat}(\text{Avg}(\text{RoIAlign}(f_V^{H'}, B))) \quad (4)$$

After the aggregation and extraction of object-level features,  $\mathbf{E}_F$  and  $\mathbf{E}_B$  are processed individually by two separate projectors ( $p_F$  and  $p_B$ ) to align with the text embeddings  $\mathbf{E}_T$ . The aligned features are then concatenated as input for LLM. We try multiple strategies to merge object-level features into visual embeddings and find the concatenation operation yields the most beneficial results. The experiments are discussed in Sec. 4.3. During training, we optimize Eq. (5) on the visual instruction tuning data to enhance the multi-modal comprehension capabilities of MG-LLaVA. For video training, we execute the aforementioned operations to each frame and then concatenate the results into an extended sequence.

$$p(\mathbf{X}_A | V_L, V_H, B, T) = \prod_{i=1}^L p_\theta(\mathbf{X}_A^{[i]} | \text{Concat}(p_F(\mathbf{E}_F), p_B(\mathbf{E}_B), \mathbf{E}_T^{[1:i-1]}), \mathbf{X}_A^{[i-1]}) \quad (5)$$

### 3.3 Training & Inference

Recently, a variety of powerful tagging models and open-vocabulary detectors have emerged, demonstrating remarkable efficacy. By using one specific tagging model to output labels, which are then used by the detector to generate bounding boxes, we can effectively avoid the generation of numerous irrelevant boxes, contrasting with the direct use of class-agnostic detectors. The details of the inference pipeline are illustrated in Appx D. For the acquisition of object bounding boxes, we employ the well-pretrained RAM [58] as the tagging model and OWL-ViT v2 [59] as detector. The generated bounding boxes are filtered by NMS and then fed to models for training and inference. It is important to note that while the RAM model aids in generating tags, these tags serve solely as inputs for the

open-vocabulary detector to determine the bounding boxes and are not integrated into the training phase.

Following LLaVA-1.5 [31], we conduct a two-stage training process. During the pretraining stage, we freeze all visual encoders and the LLM, and only train the fusion module, visual projector, and box projector. This aims to refine the fusion module’s capability to aggregate features of low and high resolutions and to enhance the projector’s alignment of visual features with the text embeddings. During instruction tuning, we keep the visual encoders frozen to maintain the integrity of high-quality image feature extraction and finetune the remaining components to enhance multi-modality comprehension.

## 4 Experiments

### 4.1 Implementation Details

**Model Settings.** In this work, all experiments are conducted based on Xtuner [60]. Specially, we choose CLIP pre-trained ViT-Large-14-336 [57] as a low-resolution visual encoder and the LAION pre-trained ConvNext-Large-320 [16] for high-resolution vision encoder. For the generation of bounding boxes, we have selected RAM-Plus [58] as the tagging model and OWL-ViT2-large-patch14-ensemble [59] as the open-vocabulary detector.

**Datasets.** During the image-based training stage, our dataset comprises 558K image-caption pairs from LAION-CCSB [61] and 708k image-caption pairs from ALLaVA-4V-Caption dataset [62], culminating in a total of 1.26M image-caption pairs for pretraining. The datasets employed for instruction-tuning encompass 665K mixture dataset from LLaVA-Instruct [31], 692k instructions from ALLaVA-4V-Instruction dataset [62], and an additional 25k instructions derived from a combination of ShareGPT4V [63], DocVQA [64], DVQA [65] and AI2D [66], with a total number of more than 1.3M image-text conversations. The superior quality of this dataset contributes to a swift enhancement in performance. For video training, following Video-LLaVA [10], we combine 558K image-text pairs and 703k video-text pairs for video pertaining. For instruction-finetuning, we utilize a 665k image-text instruction dataset from LLaVA and a 100k video-text instruction dataset from Video-ChatGPT [9].

**Training Details.** We fix all seeds across the training procedures for fairness, where we adopt the XTuner codebase [60]. We established the low-resolution parameter at 336 and the high-resolution parameter at 768. For video training, we uniformly extract 8 frames from each video. During the pretraining stage, we employ a batch size of 32 per device and an aggregate batch size of 256. In the instruction-tuning phase, we reduce the batch size to 16 per device and an overall batch size of 128. The initial learning rate is set to  $1e-3$  for the pretraining stage and  $2e-5$  for the instruction-tuning stage. The number of bounding boxes per image is limited to 100 during training. The entire training process takes approximately 23 hours when using the Vicuna7B [22] model using  $8 \times A100$  GPUs. For our most extensive model, the Yi1.5-34B [28], we utilize  $32 \times A100$  GPUs and finalize the optimization process in roughly three days by employing the DeepSpeed Zero3 strategy.

### 4.2 Main Results

**Perception Benchmarks.** In Tab. 1, we compare our MG-LLaVA with previous leading approaches across several settings on Multi-Modal benchmarks, which mainly concentrate on perception capability, including MMBench-Dev and MMBench-Test [19], SEEDBench-Image [20], and MMStar [71]. MMBench is dedicated to advancing the understanding of multi-modal perception and cognition, and SEEDBench provides a comprehensive and objective evaluation of MLLM. MMStar further ensures each selected sample exhibits visual dependency. MG-LLaVA exhibits a significantly enhanced perceptual capability compared to a wide range of MLLMs. Our MG-LLaVA equipped with phi3-3.8B [26] show superior performance than MiniCPM V2 [70] of +3.8% on both MMBench Dev and Test, and +3.1% on SEEDBench. Utilizing Vicuna-7B [22], MG-LLaVA outperforms all models with vicuna-7B and even 13B on MMBench and SEEDBench, surpassing LLaVA-1.5-7B by an average of 5.1% across four benchmarks. Moreover, with Yi1.5-34B [28], MG-LLaVA consistently outperforms GPT-4V on MMBench and SEEDBench. Concurrently, it maintains equivalent efficacy to GPT-4V

Table 1: Comparison with leading methods on several popular visual benchmarks that concentrate on perception. **Params.** denotes the total number of parameters within the model. **Res.** refers to the resolution of the input image, which is assumed to be square by default unless otherwise indicated. The notation ‘( )’ signifies the presence of both low-resolution and high-resolution inputs, with the number inside the parentheses specifying the higher resolution.

Method	LLM	Param.	Res.	MMB <sup>D</sup>	MMB <sup>T</sup>	SEED <sup>I</sup>	MMStar
<i>Private Models</i>							
GPT-4V [17]	-	-	-	75.1	77.0	72.3	49.7
GeminiProVision [18]	-	-	-	75.2	73.6	70.7	38.6
Qwen-VL-Plus [24]	-	-	-	66.2	67.0	65.7	39.7
<i>Open-source Models</i>							
BLIP-2 [67]	Vicuna-13B	14.2B	224	-	-	46.4	-
InstructBLIP [30]	Vicuna-7B	8.2B	224	-	36	53.4	-
Shikra [68]	Vicuna-13B	7.3B	224	58.8	60.2	-	-
IDEFICS-9B [69]	LLaMA-7B	-	224	48.2	45.3	-	-
IDEFICS-80B [69]	LLaMA-65B	-	224	-	54.6	-	-
Qwen-VL [24]	Qwen-7B	9.6B	448	38.2	32.2	56.3	-
Qwen-VL-Chat [24]	Qwen-7B	9.6B	448	60.6	61.8	58.2	37.5
LLaVA-1.5 [31]	Vicuna-7B	7.2B	336	65.2	66.5	66.1	30.3
LLaVA-1.5 [31]	Vicuna-13B	13.4B	336	69.2	69.2	68.2	32.8
SPHINX [12]	Vicuna-7B	10B	224	66.9	-	69.1	-
SPHINX-1k [12]	Vicuna-7B	10B	448	67.1	-	71.6	-
Mini-Gemini [8]	Vicuna-7B	7.4B	336 (768)	69.3	-	-	-
MiniCPM-V2 [70]	MiniCPM-2.4B	2.8B	448	69.6	69.1	67.1	39.1
MOVA [13]	Vicuna-7B	10B	576	70.4	-	-	-
LLaVA-HR [14]	Vicuna-13B	13.4B	448 (1024)	-	-	64.5	-
LLaVA-UHD [7]	Vicuna-13B	13.4B	672×1008	68.0	-	-	-
<i>Our Models</i>							
MG-LLaVA	Phi3-3.8B	4.2B	336 (768)	73.4	72.9	70.2	35.5
MG-LLaVA	Vicuna-7B	7.4B	336 (768)	72.1	71.9	69.4	35.1
MG-LLaVA	LLaMA3-8B	8.4B	336 (768)	76.5	76.6	71.5	36.9
MG-LLaVA	Vicuna-13B	13.6B	336 (768)	72.2	73.5	70.8	34.1
MG-LLaVA	Yi1.5-34B	34.4B	336 (768)	<b>80.1</b>	<b>79.1</b>	<b>73.7</b>	<b>47.9</b>

on MMStar. Incorporating multi-granularity visual inputs, MG-LLaVA develops its capability of capturing details within the image. More cases are exhibited in Appx. B.

**Visual Question Answering Benchmarks.** In this section, we analyze MLLM’s capability of visual conversation. The benchmarks can be divided into two groups: (1) Benchmarks require understanding the text within images to provide answers, including TextVQA(VQA<sup>T</sup>) [72] and DocVQA [73]. We report the accuracy of both validation sets. (2) General visual question answering benchmarks such as VQA-V2 [74], ScienceQA-Image(SQA<sup>I</sup>) [75], AI2D [66]. The evaluation results on VQA benchmarks are shown in Tab. 2. MG-LLaVA also demonstrates considerable proficiency on VQA benchmarks. When equipped with Vicuna-7B and 7.4B parameters, MG-LLaVA surpasses both SPHINX-1k [12], which has 10B parameters, and Mini-Gemini with 7.4B parameters on these benchmarks. Operating under identical parameter conditions, MG-LLaVA, with low-resolution input of 336 and high-resolution of 768, outperforms LLaVA-UHD [7], which incorporates an input resolution of 672×1008 on VQA<sup>T</sup>, SQA<sup>I</sup> and AI2D. MG-LLaVA exhibits its potential for expansion when integrated with larger LLM. With Yi1.5-34B [28], MG-LLaVA surpasses the majority of established baselines across a wide array of VQA benchmarks.

**Video Question Answering Benchmarks.** To demonstrate the effectiveness of our approach, we have expanded our model to encompass video comprehension. We evaluate our models on MSVD and MSRVT, and results are shown in Tab. 3. MG-LLaVA outperforms Video-LLaVA [10] on both benchmarks, which further proves the efficiency of MG-LLaVA. In video understanding, MG-LLaVA demonstrates proficiency in identifying the critical object in the video. More illustrative instances are depicted in Appx. B.

### 4.3 Ablation Experiments

In this section, we conduct comprehensive ablation studies of our model. The ablation experiments are based on the training data provided by LLaVA-1.5 [31], with a fixed seed protocol to ensure the stability and comparability of the experimental conditions.

Table 2: Comparison with laeding methods on popular VQA visual benchmarks.

Method	LLM	Param.	Res.	VQA <sup>T</sup>	DocVQA	SQA <sup>f</sup>	AI2D	VQAv2
<i>Private Models</i>								
GPT-4V	-	-	-	78.0	42.3	82.1	-	-
GeminiProVision	-	-	-	74.6	-	81.4	-	-
Qwen-VL-Plus	-	-	-	78.9	82.2	73.4	-	-
<i>Open-source Models</i>								
BLIP-2	Vicuna-13B	14.2B	224	42.5	-	61.0	-	41.0
InstructBLIP	Vicuna-7B	8.2B	224	50.1	10.9	60.5	40.6	-
Shikra	Vicuna-13B	7.3B	224	-	-	-	-	-
IDEFICS-9B	LLaMA-7B	-	224	25.9	-	-	42.2	50.9
IDEFICS-80B	LLaMA-65B	-	224	30.9	-	-	54.8	60
Qwen-VL	Qwen-7B	9.6B	448	63.8	<b>62.1</b>	67.1	57.7	78.8
Qwen-VL-Chat	Qwen-7B	9.6B	448	61.5	57.1	68.2	63	78.2
LLaVA-1.5	Vicuna-7B	7.2B	336	58.2	21.5	66.8	55.5	78.5
LLaVA-1.5	Vicuna-13B	13.4B	336	61.3	24.1	71.6	61.1	80.0
SPHINX	Vicuna-7B	10B	224	51.6	-	69.3	-	78.1
SPHINX-1k	Vicuna-7B	10B	448	58.8	-	69.1	-	80.2
Mini-Gemini	Vicuna-7B	7.4B	336(768)	65.2	-	-	-	-
LLaVA-UHD	Vicuna-13B	13.4B	672x1008	67.7	-	72.0	-	81.7
<i>Our Models</i>								
MG-LLaVA	Phi3-3.8B	4.2B	336(768)	65.3	49.3	73.9	75.1	77.9
MG-LLaVA	Vicuna-7B	7.4B	336(768)	67.3	47.9	70.8	69.3	80.2
MG-LLaVA	LLaMA3-8B	8.2B	336(768)	68.1	49.0	76.3	75.6	80.7
MG-LLaVA	Vicuna-13B	13.6B	336(768)	69.6	52.1	74.7	73.4	81.2
MG-LLaVA	Yi1.5-34B	34.4B	336(768)	<b>70.0</b>	56.1	<b>77.0</b>	<b>81.1</b>	<b>82.0</b>

Table 3: Comparison with other methods on Video-QA benchmarks.

Method	LLM	MSVD-QA	MSRVTT-QA
FrozenBiLM [76]	-	32.2	16.8
VideoChat [32]	Vicuna-7B	56.3	45.0
LLaMA-Adapter [77]	-	54.9	43.8
Video-LLaMA [78]	Vicuna-7B	51.6	29.6
Video-ChatGPT [9]	Vicuna-7B	64.9	49.3
Video-LLaVA [10]	Vicuna-7B	70.7	59.2
MG-LLaVA	Vicuna-7B	<b>71.5</b>	<b>59.8</b>

Table 4: Ablation results on MMBench-DEV [19], SEEDBench [20] and TextVQA [72]. We execute our experiments based on the LLaVA model with Vicuna-7B and Phi3-3.8B.

Object-level Features	Conv-Gate Fusion	Vicuna-7B					Phi3-3.8B				
		#TFLOPS	Params.	MMB <sup>D</sup>	SEED	VQA <sup>f</sup>	#TFLOPS	Params.	MMB <sup>D</sup>	SEED	VQA <sup>f</sup>
×	×	5.76	7.2B	68.2	64.6	56.7	3.3	4.0B	68.7	65.3	54.3
✓	×	6.20	7.4B	69.2(+1.0)	65.0(+0.4)	56.5(-0.2)	3.72	4.2B	70.4(+1.7)	66.2(+0.9)	54.5(+0.2)
✓	✓	6.21	7.4B	69.8(+1.6)	65.5(+0.9)	59.5(+2.8)	3.73	4.2B	71.0(+2.3)	66.4(+1.1)	56.8(+2.5)

**Effect of Each Component.** We first conduct ablation studies on object-level features and the Conv-Gate fusion module across multiple datasets, including MMBench-DEV [19], SEEDBench [20] and TextVQA [72]. To validate the effectiveness of our method on different scales of LLM, the baseline is built on Vicuna-7B and Phi3-3.8B. The results are shown in Tab. 4.

It is clear that the model achieves significant gains with the integration of object-level features and Conv-Gate Fusion module. When adding object-level features, the performance of MMBench-Dev, SEEDBench increases 1.0%, 0.4% separately with Vicuna-7B and 1.7%, 0.9% with Phi3. After utilizing the fusion network, the performance on these two benchmarks further increases by 1.6%, 0.9% with Vicuna-7B and 2.3%, 1.1% with Phi3. For the TextVQA benchmark, the incorporation of object-level features does not markedly enhance performance due to the suboptimal detection of textual content within images by the detector. Nevertheless, the integration of high-resolution features mitigates this limitation, culminating in an accuracy increment of 3.0% on Vicuna-7B and 2.5% on Phi3-3.8B. The integration of both modules incurs a marginal increase in computational expense and parameter count, yet it enhances the efficacy of models across various scales. We further enumerate additional comparative outcomes across various subsets of MMBench-Dev and SEEDBench, the comparative results are shown in Appx. A.



Table 5: Comparison of different fusion modules, methods of merging object-level features, and tagging models.

(a) Fusion modules.			(b) Methods of merging object-level features.			(c) Tagging models.		
Method	MMB <sup>D</sup>	MMStar	Method	MMB <sup>D</sup>	MMStar	Method	MMB <sup>D</sup>	MMStar
Baseline	69.2	34.1	Baseline	68.2	32.5	Baseline	68.2	32.5
w/ Resampler	55.6	30.5	w/ <i>F-to-B Cross Attention</i>	65.7	33.3	w/ <i>COCO80</i>	68.3	32.9
w/ Channel Concat	68.9	32.6	w/ <i>B-to-F Cross Attention</i>	67.7	34.4	w/ <i>RAM tags</i>	<b>69.2</b>	<b>34.5</b>
w/ Patch Info Mining	68.3	32.9	w/ Concat	<b>69.8</b>	<b>34.5</b>			
w/ Conv-Gate Fusion	<b>69.8</b>	<b>34.5</b>						

**Fusion Network Design.** We also explore a diverse design of fusion modules and perform ablation studies on various components: (1) *Channel Concat*. We simply concat the low and high-resolution features in the channel dimension. (2) *Patch Info Mining*. We replace the gated-fusion model with Patch Info Mining in [8]. (3) *Resampler*. We substitute the gated-fusion model with a resampler in [79]. The results are shown in Tab. 5a. We find our Conv-Gated fusion module performs better through these methods, which confirms its efficiency.

**Method of Merging Object-level Features.** We further explore various methods for incorporating object-level features: (1) *F-to-B Cross-Attention*. We add a cross-attention block to enhance the fusion features by integrating object-level features after the fusion module, the enhanced fusion features are then fed into LLM. (2) *B-to-F Cross-Attention*. Following the fusion module, another cross-attention block is employed to enhance the object-level features by integrating fusion features. The fusion features and enhanced object-level features are then concatenated as input for LLM. The frameworks of both are depicted in Appx. C and the results are reported in Tab. 5c. Our observations indicate that cross-attention does not enhance the integration of object-level features into visual representations. Conversely, concatenating object-level features with visual tokens and deferring the decision-making to the LLM yields more favorable outcomes.

**Tagging Model.** We investigate the impact of the tagging model within the bounding box generation pipeline. We compare our method with assigning fixed tags based on the 80 categories from the COCO [80] dataset to open-vocabulary detectors for producing bounding boxes. The comparative results are presented in Tab. 5b. Given that the COCO dataset’s 80 categories do not comprehensively cover real-world objects, the generated bounding boxes fail to encompass all objects within an image. This limitation consequently diminishes the impact of object-level features.

## 5 Discussions

**Conclusions** In this work, we propose MG-LLaVA, an expansive multi-modal model adept at processing visual inputs of multiple granularities, encompassing object-level features, original images, and high-resolution data. To effectively amalgamate features of varying granularities, we propose the Multi-Granularity Vision Flow module, thereby equipping the LLM with the ability to discern multi-modal interactions from a consolidated visual framework. Utilizing a range of LLMs extending from 3.8B to 34B parameters, our model exhibits pronounced scalability and remarkable performance in visual understanding, outperforming established models and significantly outperforming GPT-4V and GeminiPro Vision on benchmarks such as MMBench and SEEDBench. The validity of our methodology is substantiated through rigorous empirical studies.

**Future Works.** While MG-LLaVA attains remarkable results across various multi-modal benchmarks, it encounters challenges in effectively harnessing object features correlated with textual inputs. Our MG-LLaVA model establishes a foundational baseline for future explorations into more sophisticated techniques of integrating inputs of multiple granularities.

**Broader Impacts.** As a robust multi-modal language model, MG-LLaVA exhibits considerable prowess in visual perception and comprehension, offering an innovative methodology to further refine MLLMs. However, MG-LLaVA’s potential societal implications merit attention, as it may facilitate the creation of multimodal applications, including those with possible adverse effects. There exists a concern that MG-LLaVA could be utilized in the development of deleterious multimodal AI systems. We encourage users to carefully assess the potential impacts when deploying our model.

## References

- [1] Deyao Zhu, Jun Chen, Xiaoqian Shen, Xiang Li, and Mohamed Elhoseiny. Minigt-4: Enhancing vision-language understanding with advanced large language models. *arXiv preprint arXiv:2304.10592*, 2023. **1, 3**
- [2] Qinghao Ye, Haiyang Xu, Guohai Xu, Jiabo Ye, Ming Yan, Yiyang Zhou, Junyang Wang, Anwen Hu, Pengcheng Shi, Yaya Shi, et al. mplug-owl: Modularization empowers large language models with multimodality. *arXiv preprint arXiv:2304.14178*, 2023. **1, 3**
- [3] Haotian Liu, Chunyuan Li, Qingyang Wu, and Yong Jae Lee. Visual instruction tuning. In *NeurIPS*, 2024. **1, 2**
- [4] Hao Zhang, Hongyang Li, Feng Li, Tianhe Ren, Xueyan Zou, Shilong Liu, Shijia Huang, Jianfeng Gao, Lei Zhang, Chunyuan Li, et al. Llava-grounding: Grounded visual chat with large multimodal models. *arXiv preprint arXiv:2312.02949*, 2023. **1**
- [5] Fei Wei, Xinyu Zhang, Ailing Zhang, Bo Zhang, and Xiangxiang Chu. Lenna: Language enhanced reasoning detection assistant. *arXiv preprint arXiv:2312.02433*, 2023. **1**
- [6] Jinjin Xu, Liwu Xu, Yuzhe Yang, Xiang Li, Yanchun Xie, Yi-Jie Huang, and Yaqian Li. u-llava: Unifying multi-modal tasks via large language model. *arXiv preprint arXiv:2311.05348*, 2023. **1**
- [7] Ruyi Xu, Yuan Yao, Zonghao Guo, Junbo Cui, Zanlin Ni, Chunjiang Ge, Tat-Seng Chua, Zhiyuan Liu, Maosong Sun, and Gao Huang. Llava-uhd: an lmm perceiving any aspect ratio and high-resolution images. *arXiv preprint arXiv:2403.11703*, 2024. **1, 3, 7**
- [8] Yanwei Li, Yuechen Zhang, Chengyao Wang, Zhisheng Zhong, Yixin Chen, Ruihang Chu, Shaoteng Liu, and Jiaya Jia. Mini-gemini: Mining the potential of multi-modality vision language models. *arXiv preprint arXiv:2403.18814*, 2024. **1, 3, 7, 9**
- [9] Muhammad Maaz, Hanoona Rasheed, Salman Khan, and Fahad Shahbaz Khan. Video-chatgpt: Towards detailed video understanding via large vision and language models. *arXiv preprint arXiv:2306.05424*, 2023. **1, 6, 8**
- [10] Bin Lin, Bin Zhu, Yang Ye, Munan Ning, Peng Jin, and Li Yuan. Video-llava: Learning united visual representation by alignment before projection. *arXiv preprint arXiv:2311.10122*, 2023. **1, 3, 6, 7, 8**
- [11] Haotian Liu, Chunyuan Li, Yuheng Li, Bo Li, Yuanhan Zhang, Sheng Shen, and Yong Jae Lee. Llava-next: Improved reasoning, ocr, and world knowledge, 2024. **1, 3**
- [12] Ziyi Lin, Chris Liu, Renrui Zhang, Peng Gao, Longtian Qiu, Han Xiao, Han Qiu, Chen Lin, Wenqi Shao, Keqin Chen, et al. Sphinx: The joint mixing of weights, tasks, and visual embeddings for multi-modal large language models. *arXiv preprint arXiv:2311.07575*, 2023. **1, 7**
- [13] Zhuofan Zong, Bingqi Ma, Dazhong Shen, Guanglu Song, Hao Shao, Dongzhi Jiang, Hongsheng Li, and Yu Liu. Mova: Adapting mixture of vision experts to multimodal context. *arXiv preprint arXiv:2404.13046*, 2024. **1, 7**
- [14] Gen Luo, Yiyi Zhou, Yuxin Zhang, Xiawu Zheng, Xiaoshuai Sun, and Rongrong Ji. Feast your eyes: Mixture-of-resolution adaptation for multimodal large language models. *arXiv preprint arXiv:2403.03003*, 2024. **1, 3, 5, 7**
- [15] Xiaoyi Dong, Pan Zhang, Yuhang Zang, Yuhang Cao, Bin Wang, Linke Ouyang, Songyang Zhang, Haodong Duan, Wenwei Zhang, Yining Li, et al. Internlm-xcomposer2-4khd: A pioneering large vision-language model handling resolutions from 336 pixels to 4k hd. *arXiv preprint arXiv:2404.06512*, 2024. **1**
- [16] Christoph Schuhmann, Romain Beaumont, Richard Vencu, Cade Gordon, Ross Wightman, Mehdi Cherti, Theo Coombes, Aarush Katta, Clayton Mullis, Mitchell Wortsman, et al. Laion-5b: An open large-scale dataset for training next generation image-text models. In *NeurIPS*, 2022. **2, 5, 6**
- [17] R OpenAI. Gpt-4 technical report. arxiv 2303.08774. *View in Article*, 2(5), 2023. **2, 3, 7**
- [18] Gemini Team, Rohan Anil, Sebastian Borgeaud, Yonghui Wu, Jean-Baptiste Alayrac, Jiahui Yu, Radu Soricut, Johan Schalkwyk, Andrew M Dai, Anja Hauth, et al. Gemini: a family of highly capable multimodal models. *arXiv preprint arXiv:2312.11805*, 2023. **2, 7**
- [19] Yuan Liu, Haodong Duan, Yuanhan Zhang, Bo Li, Songyang Zhang, Wangbo Zhao, Yike Yuan, Jiaqi Wang, Conghui He, Ziwei Liu, et al. Mmbench: Is your multi-modal model an all-around player? *arXiv preprint arXiv:2307.06281*, 2023. **2, 6, 8, 16**
- [20] Bohao Li, Rui Wang, Guangzhi Wang, Yuying Ge, Yixiao Ge, and Ying Shan. Seed-bench: Benchmarking multimodal llms with generative comprehension. *arXiv preprint arXiv:2307.16125*, 2023. **2, 6, 8, 16**
- [21] Hugo Touvron, Thibaut Lavril, Gautier Izacard, Xavier Martinet, Marie-Anne Lachaux, Timothée Lacroix, Baptiste Rozière, Naman Goyal, Eric Hambro, Faisal Azhar, et al. Llama: Open and efficient foundation language models. *arXiv preprint arXiv:2302.13971*, 2023. **3**

- [22] Wei-Lin Chiang, Zhuohan Li, Zi Lin, Ying Sheng, Zhanghao Wu, Hao Zhang, Lianmin Zheng, Siyuan Zhuang, Yonghao Zhuang, Joseph E Gonzalez, et al. Vicuna: An open-source chatbot impressing gpt-4 with 90%\* chatgpt quality. See <https://vicuna.lmsys.org> (accessed 14 April 2023), 2023. 3, 6
- [23] Aiyuan Yang, Bin Xiao, Bingning Wang, Borong Zhang, Ce Bian, Chao Yin, Chenxu Lv, Da Pan, Dian Wang, Dong Yan, et al. Baichuan 2: Open large-scale language models. *arXiv preprint arXiv:2309.10305*, 2023. 3
- [24] Jinze Bai, Shuai Bai, Shusheng Yang, Shijie Wang, Sinan Tan, Peng Wang, Junyang Lin, Chang Zhou, and Jingren Zhou. Qwen-vl: A frontier large vision-language model with versatile abilities. *arXiv preprint arXiv:2308.12966*, 2023. 3, 7
- [25] InternLM Team. Internlm: A multilingual language model with progressively enhanced capabilities, 2023. 3
- [26] Marah Abdin, Sam Ade Jacobs, Ammar Ahmad Awan, Jyoti Aneja, Ahmed Awadallah, Hany Awadalla, Nguyen Bach, Amit Bahree, Arash Bakhtiari, Harkirat Behl, Alon Benhaim, Misha Bilenko, Johan Bjorck, Sébastien Bubeck, Martin Cai, Caio César Teodoro Mendes, Weizhu Chen, Vishrav Chaudhary, Parul Chopra, Allie Del Giorno, Gustavo de Rosa, Matthew Dixon, Ronen Eldan, Dan Iter, Amit Garg, Abhishek Goswami, Suriya Gunasekar, Emman Haider, Junheng Hao, Russell J. Hewett, Jamie Huynh, Mojan Javaheripi, Xin Jin, Piero Kauffmann, Nikos Karampatzakis, Dongwoo Kim, Mahoud Khademi, Lev Kurilenko, James R. Lee, Yin Tat Lee, Yanzhi Li, Chen Liang, Weishung Liu, Eric Lin, Zeqi Lin, Piyush Madan, Arindam Mitra, Hardik Modi, Anh Nguyen, Brandon Norick, Barun Patra, Daniel Perez-Becker, Thomas Portet, Reid Pryzant, Heyang Qin, Marko Radmilac, Corby Rosset, Sambudha Roy, Olatunji Ruwase, Olli Saarikivi, Amin Saied, Adil Salim, Michael Santacrose, Shital Shah, Ning Shang, Hiteshi Sharma, Xia Song, Masahiro Tanaka, Xin Wang, Rachel Ward, Guanhua Wang, Philipp Witte, Michael Wyatt, Can Xu, Jiahang Xu, Sonali Yadav, Fan Yang, Ziyi Yang, Donghan Yu, Chengruidong Zhang, Cyril Zhang, Jianwen Zhang, Li Lyna Zhang, Yi Zhang, Yue Zhang, Yunan Zhang, and Xiren Zhou. Phi-3 technical report: A highly capable language model locally on your phone, 2024. 3, 6
- [27] AI@Meta. Llama 3 model card. 2024. 3
- [28] Alex Young, Bei Chen, Chao Li, Chengen Huang, Ge Zhang, Guanwei Zhang, Heng Li, Jiangcheng Zhu, Jianqun Chen, Jing Chang, et al. Yi: Open foundation models by 01. ai. *arXiv preprint arXiv:2403.04652*, 2024. 3, 6, 7
- [29] Zhe Chen, Jiannan Wu, Wenhai Wang, Weijie Su, Guo Chen, Sen Xing, Zhong Muyan, Qinglong Zhang, Xizhou Zhu, Lewei Lu, et al. Internvl: Scaling up vision foundation models and aligning for generic visual-linguistic tasks. *arXiv preprint arXiv:2312.14238*, 2023. 3
- [30] Wenliang Dai, Junnan Li, Dongxu Li, Anthony Meng Huat Tiong, Junqi Zhao, Weisheng Wang, Boyang Li, Pascale N Fung, and Steven Hoi. Instructblip: Towards general-purpose vision-language models with instruction tuning. In *NeurIPS*, 2024. 3, 7
- [31] Haotian Liu, Chunyuan Li, Yuheng Li, and Yong Jae Lee. Improved baselines with visual instruction tuning. *arXiv preprint arXiv:2310.03744*, 2023. 3, 5, 6, 7
- [32] KunChang Li, Yinan He, Yi Wang, Yizhuo Li, Wenhai Wang, Ping Luo, Yali Wang, Limin Wang, and Yu Qiao. Videochat: Chat-centric video understanding. *arXiv preprint arXiv:2305.06355*, 2023. 3, 8
- [33] Tao Zhang, Xiangtai Li, Hao Fei, Haobo Yuan, Shengqiong Wu, Shunping Ji, Change Loy Chen, and Shuicheng Yan. Omg-llava: Bridging image-level, object-level, pixel-level reasoning and understanding. *arXiv preprint*, 2024. 3
- [34] Kuan-Chih Huang, Xiangtai Li, Lu Qi, Shuicheng Yan, and Ming-Hsuan Yang. Reason3d: Searching and reasoning 3d segmentation via large language model. *arXiv*, 2024. 3
- [35] Shengqiong Wu, Hao Fei, Xiangtai Li, Jiayi Ji, Hanwang Zhang, Tat-Seng Chua, and Shuicheng Yan. Towards semantic equivalence of tokenization in multimodal llm. *arXiv preprint arXiv:2406.05127*, 2024. 3
- [36] Zhang Li, Biao Yang, Qiang Liu, Zhiyin Ma, Shuo Zhang, Jingxu Yang, Yabo Sun, Yuliang Liu, and Xiang Bai. Monkey: Image resolution and text label are important things for large multi-modal models. *arXiv preprint arXiv:2311.06607*, 2023. 3
- [37] Pan Zhang, Xiaoyi Dong Bin Wang, Yuhang Cao, Chao Xu, Linke Ouyang, Zhiyuan Zhao, Shuangrui Ding, Songyang Zhang, Haodong Duan, Hang Yan, et al. Internlm-xcomposer: A vision-language large model for advanced text-image comprehension and composition. *arXiv preprint arXiv:2309.15112*, 2023. 3
- [38] Qijie Zhao, Tao Sheng, Yongtao Wang, Zhi Tang, Ying Chen, Ling Cai, and Haibin Ling. M2det: A single-shot object detector based on multi-level feature pyramid network. In *AAAI*, 2019. 3
- [39] Rui Qian, Yuxi Li, Huabin Liu, John See, Shuangrui Ding, Xian Liu, Dian Li, and Weiyao Lin. Enhancing self-supervised video representation learning via multi-level feature optimization. In *ICCV*, 2021. 3

- [40] Shilong Liu, Zhaoyang Zeng, Tianhe Ren, Feng Li, Hao Zhang, Jie Yang, Chunyuan Li, Jianwei Yang, Hang Su, Jun Zhu, et al. Grounding dino: Marrying dino with grounded pre-training for open-set object detection. *arXiv preprint arXiv:2303.05499*, 2023. 3
- [41] Bo Wan, Desen Zhou, Yongfei Liu, Rongjie Li, and Xuming He. Pose-aware multi-level feature network for human object interaction detection. In *ICCV*, 2019. 3
- [42] Xiangtai Li, Haobo Yuan, Wei Li, Henghui Ding, Size Wu, Wenwei Zhang, Yining Li, Kai Chen, and Chen Change Loy. Omg-seg: Is one model good enough for all segmentation? In *CVPR*, 2024. 3
- [43] Haobo Yuan, Xiangtai Li, Chong Zhou, Yining Li, Kai Chen, and Chen Change Loy. Open-vocabulary sam: Segment and recognize twenty-thousand classes interactively. *arXiv preprint*, 2024. 3
- [44] Chong Zhou, Xiangtai Li, Chen Change Loy, and Bo Dai. Edgesam: Prompt-in-the-loop distillation for on-device deployment of sam. *arXiv preprint arXiv:2312.06660*, 2023. 3
- [45] Daan de Geus, Panagiotis Meletis, and Gijs Dubbelman. Single network panoptic segmentation for street scene understanding. In *IV*, 2019. 3
- [46] Alexander Kirillov, Ross Girshick, Kaiming He, and Piotr Dollár. Panoptic feature pyramid networks. In *CVPR*, 2019. 3
- [47] Yanwei Li, Xinze Chen, Zheng Zhu, Lingxi Xie, Guan Huang, Dalong Du, and Xingang Wang. Attention-guided unified network for panoptic segmentation. In *CVPR*, 2019. 3
- [48] Shilin Xu, Xiangtai Li, Jingbo Wang, Guangliang Cheng, Yunhai Tong, and Dacheng Tao. Fashionformer: A simple, effective and unified baseline for human fashion segmentation and recognition. *ECCV*, 2022. 3
- [49] Vignesh Ramanathan, Anmol Kalia, Vladan Petrovic, Yi Wen, Baixue Zheng, Baishan Guo, Rui Wang, Aaron Marquez, Rama Kovvuri, Abhishek Kadian, et al. Paco: Parts and attributes of common objects. In *CVPR*, 2023. 3
- [50] Lu Qi, Yi-Wen Chen, Lehan Yang, Tiancheng Shen, Xiangtai Li, Weidong Guo, Yu Xu, and Ming-Hsuan Yang. Generalizable entity grounding via assistance of large language model. *arXiv preprint arXiv:2402.02555*, 2024. 3
- [51] Umberto Michieli, Edoardo Borsato, Luca Rossi, and Pietro Zanuttigh. Gmnet: Graph matching network for large scale part semantic segmentation in the wild. In *ECCV*, 2020. 3
- [52] Yifan Zhao, Jia Li, Yu Zhang, and Yonghong Tian. Multi-class part parsing with joint boundary-semantic awareness. In *ICCV*, 2019. 3
- [53] Daan de Geus, Panagiotis Meletis, Chenyang Lu, Xiaoxiao Wen, and Gijs Dubbelman. Part-aware panoptic segmentation. In *CVPR*, 2021. 3
- [54] Xiangtai Li, Shilin Xu, Yibo Yang, Guangliang Cheng, Yunhai Tong, and Dacheng Tao. Panoptic-partformer: Learning a unified model for panoptic part segmentation. In *ECCV*, 2022. 3
- [55] Xiangtai Li, Shilin Xu, Yibo Yang, Haobo Yuan, Guangliang Cheng, Yunhai Tong, Zhouchen Lin, Ming-Hsuan Yang, and Dacheng Tao. Panopticpartformer++: A unified and decoupled view for panoptic part segmentation. *arXiv preprint arXiv:2301.00954*, 2023. 3
- [56] Alexander Kirillov, Eric Mintun, Nikhila Ravi, Hanzi Mao, Chloe Rolland, Laura Gustafson, Tete Xiao, Spencer Whitehead, Alexander C Berg, Wan-Yen Lo, et al. Segment anything. In *ICCV*, 2023. 3
- [57] Alec Radford, Jong Wook Kim, Chris Hallacy, Aditya Ramesh, Gabriel Goh, Sandhini Agarwal, Girish Sastry, Amanda Askell, Pamela Mishkin, Jack Clark, et al. Learning transferable visual models from natural language supervision. In *ICML*, 2021. 5, 6
- [58] Youcai Zhang, Xinyu Huang, Jinyu Ma, Zhaoyang Li, Zhaochuan Luo, Yanchun Xie, Yuzhuo Qin, Tong Luo, Yaqian Li, Shilong Liu, et al. Recognize anything: A strong image tagging model. *arXiv preprint arXiv:2306.03514*, 2023. 5, 6
- [59] Matthias Minderer, Alexey Gritsenko, and Neil Houlsby. Scaling open-vocabulary object detection. In *NeurIPS*, 2024. 5, 6
- [60] XTuner Contributors. Xtuner: A toolkit for efficiently fine-tuning llm. <https://github.com/InternLM/xtuner>, 2023. 6
- [61] Piyush Sharma, Nan Ding, Sebastian Goodman, and Radu Soricut. Conceptual captions: A cleaned, hypernymed, image alt-text dataset for automatic image captioning. In *Proceedings of the 56th Annual Meeting of the Association for Computational Linguistics (Volume 1: Long Papers)*, 2018. 6
- [62] Guiming Hardy Chen, Shunian Chen, Ruifei Zhang, Junying Chen, Xiangbo Wu, Zhiyi Zhang, Zhihong Chen, Jianquan Li, Xiang Wan, and Benyou Wang. Allava: Harnessing gpt4v-synthesized data for a lite vision-language model. *arXiv preprint arXiv:2402.11684*, 2024. 6
- [63] Lin Chen, Jisong Li, Xiaoyi Dong, Pan Zhang, Conghui He, Jiaqi Wang, Feng Zhao, and Dahua Lin. Sharegpt4v: Improving large multi-modal models with better captions. *arXiv preprint arXiv:2311.12793*, 2023. 6

- [64] Rubèn Tito, Dimosthenis Karatzas, and Ernest Valveny. Document collection visual question answering. In *ICDAR*, 2021. 6
- [65] Kushal Kafle, Brian Price, Scott Cohen, and Christopher Kanan. Dvqa: Understanding data visualizations via question answering. In *CVPR*, 2018. 6
- [66] Aniruddha Kembhavi, Mike Salvato, Eric Kolve, Minjoon Seo, Hannaneh Hajishirzi, and Ali Farhadi. A diagram is worth a dozen images. In *ECCV*. Springer, 2016. 6, 7
- [67] Junnan Li, Dongxu Li, Silvio Savarese, and Steven Hoi. Blip-2: Bootstrapping language-image pre-training with frozen image encoders and large language models. In *ICML*. PMLR, 2023. 7
- [68] Keqin Chen, Zhao Zhang, Weili Zeng, Richong Zhang, Feng Zhu, and Rui Zhao. Shikra: Unleashing multimodal llm’s referential dialogue magic. *arXiv preprint arXiv:2306.15195*, 2023. 7
- [69] Hugo Laurençon, Lucile Saulnier, Léo Tronchon, Stas Bekman, Amanpreet Singh, Anton Lozhkov, Thomas Wang, Siddharth Karamcheti, Alexander Rush, Douwe Kiela, et al. Obelics: An open web-scale filtered dataset of interleaved image-text documents. In *NeurIPS*, 2024. 7
- [70] Shengding Hu, Yuge Tu, Xu Han, Chaoqun He, Ganqu Cui, Xiang Long, Zhi Zheng, Yewei Fang, Yuxiang Huang, Weilin Zhao, et al. Minicpm: Unveiling the potential of small language models with scalable training strategies. *arXiv preprint arXiv:2404.06395*, 2024. 6, 7
- [71] Lin Chen, Jinsong Li, Xiaoyi Dong, Pan Zhang, Yuhang Zang, Zehui Chen, Haodong Duan, Jiaqi Wang, Yu Qiao, Dahua Lin, et al. Are we on the right way for evaluating large vision-language models? *arXiv preprint arXiv:2403.20330*, 2024. 6
- [72] Amanpreet Singh, Vivek Natarajan, Meet Shah, Yu Jiang, Xinlei Chen, Dhruv Batra, Devi Parikh, and Marcus Rohrbach. Towards vqa models that can read. In *CVPR*, 2019. 7, 8, 16
- [73] Minesh Mathew, Dimosthenis Karatzas, and CV Jawahar. Docvqa: A dataset for vqa on document images. In *WACV*, 2021. 7
- [74] Stanislaw Antol, Aishwarya Agrawal, Jiasen Lu, Margaret Mitchell, Dhruv Batra, C Lawrence Zitnick, and Devi Parikh. Vqa: Visual question answering. In *ICCV*, 2015. 7
- [75] Pan Lu, Swaroop Mishra, Tanglin Xia, Liang Qiu, Kai-Wei Chang, Song-Chun Zhu, Oyvind Tafjord, Peter Clark, and Ashwin Kalyan. Learn to explain: Multimodal reasoning via thought chains for science question answering. In *NeurIPS*, 2022. 7
- [76] Antoine Yang, Antoine Miech, Josef Sivic, Ivan Laptev, and Cordelia Schmid. Zero-shot video question answering via frozen bidirectional language models. In *NeurIPS*, 2022. 8
- [77] Renrui Zhang, Jiaming Han, Chris Liu, Peng Gao, Aojun Zhou, Xiangfei Hu, Shilin Yan, Pan Lu, Hongsheng Li, and Yu Qiao. Llama-adapter: Efficient fine-tuning of language models with zero-init attention. *arXiv preprint arXiv:2303.16199*, 2023. 8
- [78] Hang Zhang, Xin Li, and Lidong Bing. Video-llama: An instruction-tuned audio-visual language model for video understanding. *arXiv preprint arXiv:2306.02858*, 2023. 8
- [79] Jean-Baptiste Alayrac, Jeff Donahue, Pauline Luc, Antoine Miech, Iain Barr, Yana Hasson, Karel Lenc, Arthur Mensch, Katherine Millican, Malcolm Reynolds, et al. Flamingo: a visual language model for few-shot learning. In *NeurIPS*, 2022. 9
- [80] Tsung-Yi Lin, Michael Maire, Serge Belongie, James Hays, Pietro Perona, Deva Ramanan, Piotr Dollár, and C Lawrence Zitnick. Microsoft coco: Common objects in context. In *ECCV*, 2014. 9

## A Appendix / Detailed results on subsets

In this section, we compare the influence of object-level features on several subsets of MMBench-Dev and Seed-bench, as shown in Fig. 4. It can be observed that the integration of object-level features significantly enhances the model’s capability in multiple aspects of perception including Attribute Reasoning, Fine-grained Perception, Physical Relation Perception, Visual Reasoning, *etc.*

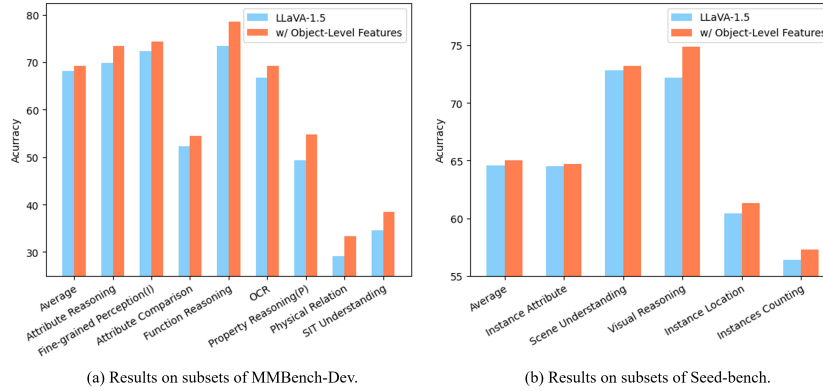


Figure 4: Ablation study on several subsets of MMBench-DEV-EN and Seed-bench. Fine-grained Perception(I) denotes *Fine-grained Perception(instance-level)*, Property Reasoning(P) means *Property Reasoning Perception* and SIT Understanding denotes *Structuralized Image-Text Understanding*.

## B Appendix / Additional Showcases

In this section, we present additional instances to substantiate the capability of MG-LLaVA. As presented in Fig. 5 and Fig. 6, MG-LLaVA is proficient in addressing queries that necessitate meticulous attention to specifics and in capturing fine-grained details within image or video. These further instances reinforce the superior performance of our MG-LLaVA in visual comprehension.

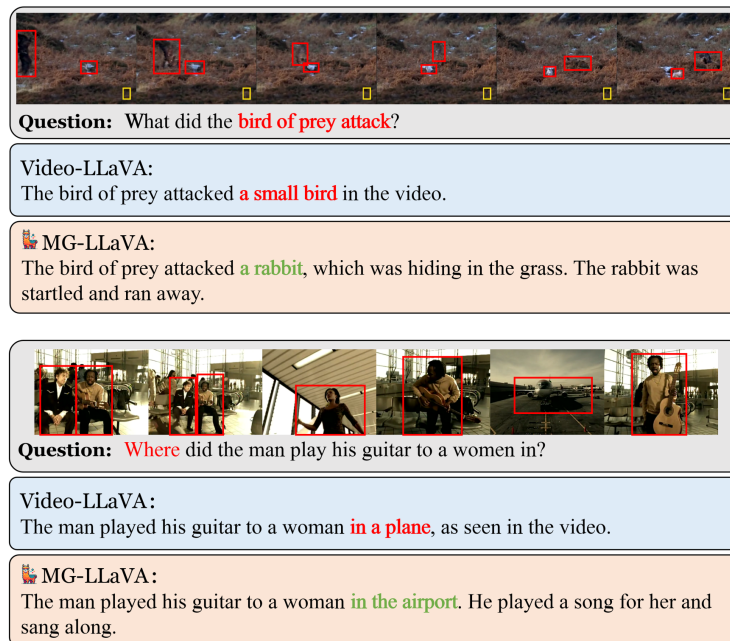


Figure 5: More cases of video understanding.



Figure 6: More cases of image understanding.

## C Appendix / Method of Merging Object-level Features

The illustration of *F-to-B Cross-Attention* and *B-to-F Cross-Attention* is depicted in Fig. 7.

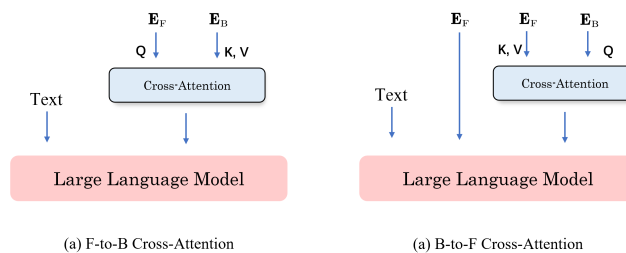


Figure 7: Illustration of F-to-B Cross-Attention and B-to-F Cross-Attention.

## D Appendix / Inference Pipeline

The inference pipeline of MG-LLaVA is displayed in Fig. 8. The tagging model first processes the input image to provide tags within the image, which are subsequently utilized as the text input of the detector to derive bounding boxes corresponding to the tagged objects within the image.

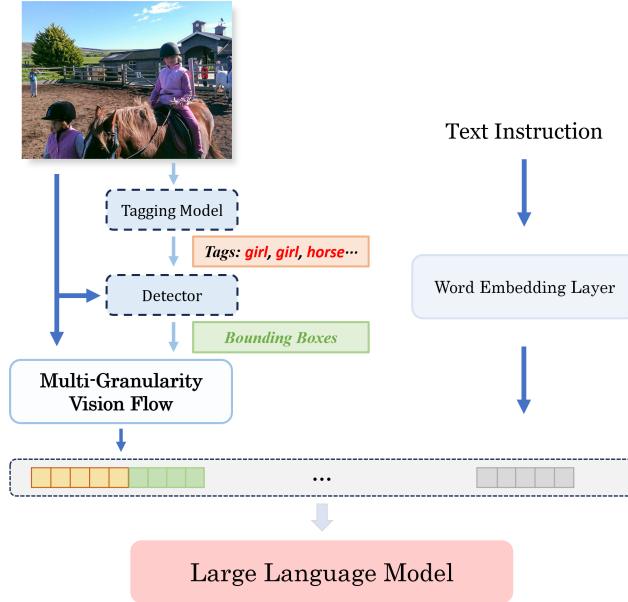


Figure 8: Inference pipeline of MG-LLaVA.

## E Appendix / Comparison of Tagging Models

Table 6: Ablation results on MMBench-DEV [19], SEEDBench [20] and TextVQA [72]. We execute our experiments based on the LLaVA model with Vicuna-7B and Phi3-3.8B.

Method	Images	Number of Boxes					
		0	1-10	12-20	21-30	30-50	>50
COCO 80 + OWL-ViT v2	389722	71118	245952	44059	28593	0	0
RAM + OWL-ViT v2	389722	43654	184706	91245	34648	22827	12645